Parthenolide Inhibits Tubulin Carboxypeptidase Activity

Xavier Fonrose,[1] Frédéric Ausseil,[2] Emmanuelle Soleilhac,[1] Véronique Masson,[2] Bruno David,[3] Isabelle Pouny,[3] Jean-Christophe Cintrat,[4] Bernard Rousseau,[4] Caroline Barette,[1] Georges Massiot,[3] and Laurence Lafanechère[1]

[1]Centre de Criblage pour Molécules Bio-Actives, institut de Recherches en Technologies et Sciences pour le Vivant, Commissariat à l'Energie Atomique-Grenoble, Grenoble, France; [2]Centre de Criblage Pharmacologique, Centre National de la Recherche Scientifique-Pierre Fabre Joint Service Unit #2646, Institut de Sciences et Technologies du Médicament de Toulouse; [3]Chimie des Substances Naturelles Bio-Actives, Centre National de la Recherche Scientifique-Pierre Fabre Joint Service Unit #2597, Institut de Sciences et Technologies du Médicament de Toulouse, Toulouse, France; and [4]Service de Marquage Moléculaire et de Chimie Bioorganique, institut de Biologie et de Technologies de Saclay, Commissariat à l'Energie Atomique-Saclay, Gif sur Yvette, France

Abstract

Microtubules are centrally involved in cell division, being the principal components of mitotic spindle. Tubulin, the constituent of microtubules, can be cyclically modified on its α-subunit by enzymatic removal of the COOH-terminal tyrosine residue by an ill-defined tubulin carboxypeptidase (TCP) and its readdition by tubulin tyrosine ligase (TTL). We and others have previously shown that suppression of TTL and resulting accumulation of detyrosinated tubulin are frequent in human cancers of poor prognosis. Explanations for the involvement of TTL and detyrosinated tubulin in tumor progression arise from the recent discovery that tubulin detyrosination leads to CAP-Gly protein mislocalization, which correlates with defects in spindle positioning during mitosis. Impaired control of spindle positioning is one factor favoring tumor invasiveness. Thus, TCP could be a target for developing novel therapeutic strategies against advanced stages of cancers. Inhibitors of TCP, by reversing abnormal detyrosinated tubulin accumulation in tumor cells, could impair tumor progression. TCP has never been isolated and this has hampered search of specific inhibitors. In this article, we describe a cell-based assay of TCP activity and its use to screen a library of natural extracts for their inhibitory potency. This led to the isolation of two sesquiterpene lactones. We subsequently found that parthenolide, a structurally related compound, can efficiently inhibit TCP. This inhibitory activity is a new specific property of parthenolide independent of its action on the nuclear factor-κB pathway. Parthenolide is also known for its anticancer properties. Thus, TCP inhibition could be one of the underlying mechanisms of these anticancer properties. [Cancer Res 2007;67(7):3371–8]

Introduction

Microtubules are key components of the cytoskeleton of eukaryotic cells. They are centrally involved in the control and mechanics of cell division, being the principal components of mitotic spindle. The building block of microtubules is the αβ-tubulin heterodimer. In most eukaryotic cells, the α chain of tubulin can be modified by enzymatic removal of the COOH-terminal tyrosine residue by an ill-defined tubulin carboxypeptidase (TCP) and by readdition of this tyrosine by a distinct enzyme, tubulin tyrosine ligase (TTL; refs. 1, 2). This tyrosination cycle is conserved among eukaryotes (1, 3) and generates two tubulin pools: intact tyrosinated α-tubulin (Tyr-tubulin) and detyrosinated α-tubulin (Glu-tubulin), which lacks the COOH-terminal tyrosine. Its physiologic importance in normal cells, tissues, or organisms has been shown with the generation of TTL-null mice. TTL-null mice die within hours after birth due to the disorganization of vital neuronal circuits (4), indicating that TTL is essential for neuronal organization.

TTL is also frequently suppressed during tumor progression (5), with resulting accumulation of Glu-tubulin in tumor cells. TTL suppression and resulting tubulin detyrosination in human cancers are associated with increased tumor aggressiveness (6–8). Experiments conducted in yeast (9), in TTL nude mice (4), and in TTL-null fibroblasts (10) show that tubulin tyrosination regulates microtubule interactions with CAP-Gly microtubule plus tip-tracking proteins, such as CLIP-170. In TTL-null fibroblasts, tubulin detyrosination and CAP-Gly protein mislocalization correlate with defects in spindle positioning during mitosis. Because impaired control of spindle positioning has previously been proposed as one factor favoring tumor invasiveness (11), these results partly shed light on the molecular basis for the apparent stimulatory effect of Glu-tubulin accumulation on tumor progression.

Inhibition of TCP could reverse abnormal Glu-tubulin accumulation in tumor cells and could lead to the restoration of normal Tyr-tubulin levels through tubulin synthesis (4). Such an inhibition could thus impair tumor progression (7, 8). Until now, there are no known specific TCP inhibitors (12). Moreover, the *TCP* gene has never been identified, although biochemical TCP activity has been reported to be present in some subcellular fractions (1, 3). Thus, the discovery of specific TCP inhibitors could also be useful for a ligand-based affinity purification of TCP. Finally, TCP inhibition is also necessary for a full understanding of the tyrosination cycle. Detyrosinated tubulin is very abundant in differentiated cells (13). Although tubulin tyrosination is essential for microtubule interaction with some proteins plus tip-tracking proteins, it is not known why eukaryotic cells developed a tyrosination cycle by introducing a detyrosination reaction.

Chemogenomic strategies have proven useful to isolate chemical compounds that could induce a specific phenotype (14, 15). In such approaches, also referred as chemical genetics, cells are tested against a library of small molecules using high-throughput screening and then examined for a desired phenotype (16–18). The subsequent identification of the intracellular protein target of

Requests for reprints: Laurence Lafanechère, Centre de Criblage pour Molécules Bio-Actives, institut de Recherches en Technologies et Sciences pour le Vivant, Commissariat à l'Energie Atomique-Grenoble, 17 Rue des Martyrs, 38054 Grenoble, France. Phone: 33-438-78-6671; Fax: 33-438-78-5032; E-mail: laurence.lafanechere@cea.fr.

doi:10.1158/0008-5472.CAN-06-3732

these compounds, although often technically difficult (19), has obtained notable successes (20–23). We designed a phenotype assay of TCP activity and used this cell-based assay to screen a chemical library to isolate TCP inhibitors. In this report, we describe the assay, its application to a screen of 23,904 natural extracts, and the purification and characterization of two sesquiterpene lactones that were able to specifically inhibit TCP. We tested several structurally related compounds and found that parthenolide, a known nuclear factor-κB (NF-κB) inhibitor (24), can efficiently inhibit TCP activity. Parthenolide has also been shown to present some anticancer properties, but the underlying mechanisms are not fully understood. TCP inhibition could be one of the mechanisms underlying the known anticancer properties of parthenolide.

Materials and Methods

Cell Culture

HeLa cells were purchased from the American Type Culture Collection (Rockville, MD). They were grown in RPMI 1640 with Glutamax supplemented with 10% fetal bovine serum (FBS) and 1% penicillin-streptomycin. Cells were maintained at 37°C in 5% CO_2 and 95% air.

Reagents

Carboxypeptidase A (CPA), orthophenanthroline, bovine serum albumin (BSA), EGTA, DMSO, glycerol, Hoechst 33258, magnesium chloride solution, PIPES, potassium chloride, potassium phosphate monobasic, sodium phosphate dibasic, Triton X-100, and Tween 20 were purchased from Sigma-Aldrich (St. Louis, MO). RPMI 1640 with Glutamax I, trypsin-EDTA solution, and penicillin-streptomycin solution was from Life Technologies, Invitrogen (Carlsbad, CA). Sodium chloride was from Carlo Erba Reagents (Rodano, Milan, Italy). FBS was from Perbio (Brebières, France). SuperSignal ELISA Pico chemiluminescent substrate was from Pierce (Rockford, IL).

Chemical Compounds

Parthenolide and costunolide were from Chromadex (Santa Ana, CA). 1N-02620, 1N-20266, 1N-21474, 1N-24000, 1N-24632, and 1N-37712 were from InterBioScreen (Moscow, Russia). Epoxyastaphiatone, alantolactone, and arglabine were from Specs (Delft, the Netherlands). Ergolide, deacetylmatricarin, and helenalin were from Apin Chemicals (Abingdon, United Kingdom). Santonin and sulindac were from Sigma-Aldrich (L'Isle d'Abeau, Chesnes, France). Cnicin was from Roth-Sochiel (Lauterbourg, France).

Dihydroparthenolide was obtained by hydrogenation of parthenolide as described by Kwok et al. (25).

Antibodies

The monoclonal ID3 (TTL blocking antibody) and the monoclonal Tyr-tubulin antibody (clone YL1/2) were generous gifts from Dr. J. Wehland (National Research Centre for Biotechnology, Braunschweig, Germany) and Dr. J.V. Kilmartin (Medical Research Council, Cambridge, United Kingdom), respectively. YL1/2 can also be purchased from Abcam (Cambridge, United Kingdom).[5] The polyclonal Glu-tubulin antibody (L4) was produced in our laboratory and is also commercially available from Abcys (Paris, France). The anti-rabbit horseradish peroxidase (HRP)-conjugated antibody and the anti-rabbit and anti-mouse cyanine 3 (Cy3)-conjugated antibodies were from Jackson ImmunoResearch Laboratories (West Grove, PA). The Alexa Fluor 488–conjugated goat antibody was from Molecular Probes (Invitrogen Corp., Carlsbad, CA).

96-Well Format Assay of TCP Activity

Microplate preparation. HeLa cells were cultured as monolayers. The cells were seeded at 30,000 per well in 96-well polystyrene tissue culture plates (reference no. 655 083; Greiner Bio-One, Kremsmuenster, Austria) in 90 μL medium. They were allowed to grow for 24 h.

Drug addition. The day following microplate preparation, each well was robotically supplemented with 10 μL RPMI 1640 containing natural extracts and paclitaxel so that the final concentrations were 35 μg/mL for natural extracts and 5 μmol/L for paclitaxel. Bioinactive controls were obtained with paclitaxel alone (5 μmol/L). The final concentration of DMSO was 0.5%. After drugs dispense, cells were incubated for 2 h at 37°C, 5% CO_2, in the workstation incubator.

Cell immunostaining. After medium aspiration, cells were washed with TBS/0.1% Tween 20 and fixed for 1 h with 3.7% formaldehyde. Cells were permeabilized with 100 μL methanol for 5 min.

After two washes with 300 μL of TBS/0.03% Tween 20 [10 mmol/L Tris-HCl, 137 mmol/L NaCl, 0.03% (v/v) Tween 20 (pH 7.4)], cells were coincubated for 1.5 h at 37°C with Glu-tubulin and HRP-conjugated antibodies diluted, respectively, at 1:10,000 and 1:5,000. Cells were rinsed twice and then incubated for 10 min with SuperSignal ELISA Pico chemiluminescent substrate. Luminescence was measured using a BMG FLUOstar Optima plate reader (BMG Labtechnologies, Offenburg, Germany).

Result analysis. Raw data were exported from the software of the microplate reader to an Excel file and normalized according to the following procedure. Mean values of DMSO and paclitaxel were calculated for each individual microplate using intraplate control data points. Paclitaxel and DMSO mean values were considered as bioinactive control (0% inhibition) and bioactive control (100% inhibition) of TCP activity, respectively.

Assay performance. To evaluate the quality of the assay, the Z′ factor was calculated using the following equation according to Zhang et al. (26):

$$Z' = 1 - \frac{(3\sigma_{c+} + 3\sigma_{c-})}{|\mu_{c+} - \mu_{c-}|}$$

where c^+ is the bioactive controls, c^- is the bioinactive controls, μ is the mean, and σ is the SD.

In our experimental conditions, the Z′ was comprised between 0.54 and 0.57, indicating that the assay is of good quality for high-throughput screening.

Sample Collection and Extract Preparation

Plant samples were collected worldwide under the general framework of the International Convention on Biological Diversity (Rio de Janeiro, Argentina, 1992). Bases for the collection were the taxonomic identification of the species, botanical diversity, and availability for a second collection. No rare or protected plants belonged to the collection. When possible, the different organs of the plants were separated and treated as different samples (bark, leaves, root, etc.). Each plant sample was dried (55°C) and finely ground. An aliquot of the plant (20 g) was macerated overnight in 200 mL ethyl acetate in an Erlenmeyer flask; after filtration, the solvent was evaporated in vacuo to give the ethyl acetate crude extract. Part of the extract (50 mg) was adsorbed on 500 mg Sigel, which was placed on top of SiO_2 solid-phase extraction cartridge. Successive elutions with $CHCl_3$, $CHCl_3$/MeOH (17:3), and MeOH provided three "fractions," which were conditioned in 96-well deep-well plates for the screening after evaporation of the solvents and replacement with 1 mL DMSO, along with the "crude extract" at a concentration of 50 mg/mL.

Bioassay-Guided Fractionation of the Extract from *Vernonia perrottetii*

Finely ground aerial parts from the plant (97 g) were macerated overnight in 1 L ethyl acetate; the suspension was filtered and the organic filtrate was evaporated in vacuum to give 9.6 g of a gum. Part of this extract (4 g) was dissolved in 8 mL chloroform and adsorbed on a Sigel column (120 g) eluted in 200 mL fractions under 18 p.s.i. at a 30 mL/min flow rate with a chloroform/methanol gradient (10 min: $CHCl_3$; 50 min: $CHCl_3$/MeOH (17:3); 10 min: MeOH). The second fraction concentrated the activity and was further purified on a semiprep high-performance liquid chromatography

[5] http://www.abcam.com

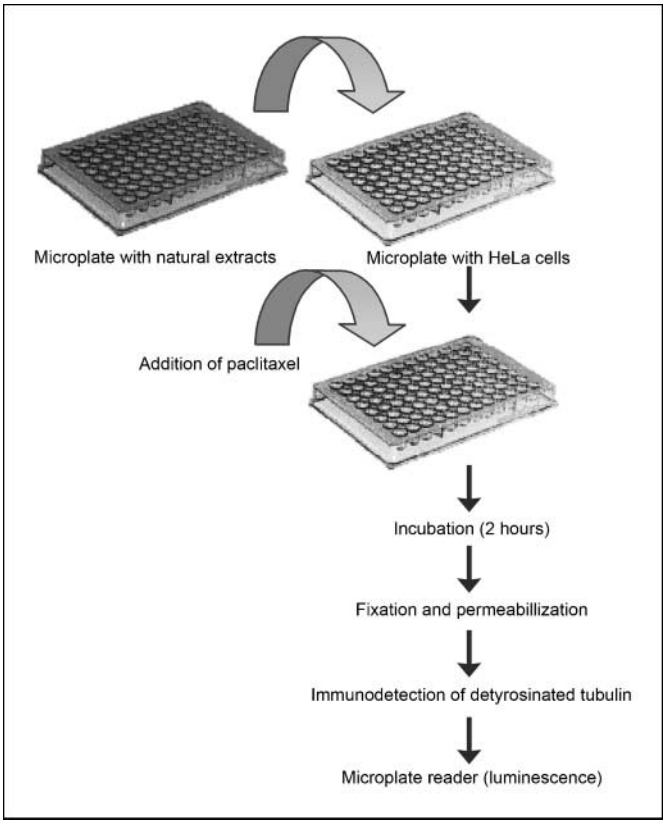

Figure 1. Schematic illustration of the different steps of the cell-based assay of TCP activity used for high-throughput screening of TCP inhibitors. TCP activity on paclitaxel-stabilized microtubules is measured by quantifying the production of detyrosinated tubulin using a specific antibody and an immunoluminescence procedure as described in Materials and Methods. The inhibitory effect of active natural extracts is detected by a decrease of the luminescent signal.

Lichrospher column with a water/acetonitrile gradient. Compound V18 was eluted at 15.6 min and compound V19 was eluted at 16.6 min (gradient system: water/acetonitrile, from 6/4 to 1/19 in 20 min).

Description of the Molecules

V18: crystals from diethyl ether (melting point 136°C), MS, UV, IR, and nuclear magnetic resonance (NMR) spectra identical with those published in the literature (27); V19: amorphous gum with MS, UV, IR, and NMR spectra identical with those published in the literature.

Cytotoxicity Assay

Some of the natural extract fractions were tested for their cytotoxic activity. This cytotoxic activity was estimated using 3-(4,5-dimethylthiazol-2-yl)-2,5-diphenyltetrazolium bromide (MTT) cell proliferation/cytotoxicity assay. This assay is a colorimetric assay, which measures the reduction of a tetrazolium component (MTT) into an insoluble formazan product by the mitochondria of viable cells. Briefly, cells were plated in 96-well flat-bottomed microplates at a density of 30,000 per well. Twenty-four hours after plating, the fractions were added and appropriately diluted in DMSO. After 2 h of incubation with the fractions, the medium was replaced with MTT (Sigma-Aldrich) dissolved at a final concentration of 1 mg/mL in serum-free, phenol red–free RPMI 1640 (Life Technologies). The cells were then let to incubate for 3 h to develop purple formazan precipitate. The MTT formazan was then solubilized in DMSO, and the absorbance was measured at a wavelength of 570 nm and a reference wavelength of 630 nm.

Immunofluorescence Procedure

Cells grown for 2 days on glass coverslips were washed with warm PBS and fixed for 6 min in anhydrous methanol at −20°C. After an additional wash in PBS/0.1% (v/v) Tween 20, cells were sequentially incubated with primary antibodies and appropriate secondary antibodies. Antibodies were diluted in PBS/0.1% BSA. YL1/2 and L4 antibodies were used at a 1:4,000 dilution. Cy3-conjugated antibodies and Alexa Fluor 488–conjugated antibodies were used at a 1:1,000 and 1:500 dilution, respectively. Nuclei were stained with Hoechst 33258 (1 μg/mL).

Coverslips were mounted in FluorSave and observed using a Zeiss Axioskop microscope (Zeiss, Oberkochen, Germany).

Microinjection

Cells grown on glass coverslips were injected using a 5171 micromanipulator and a 5246 transjector (Eppendorf-Netheler-Hinz GmbH, Hamburg, Germany).

ID3 antibody used in microinjection experiments was diluted at a concentration of 4 mg/mL in PBS buffer. Before microinjection, the solution was clarified by centrifugation in a Beckman TLA-100 rotor (100,000 × *g*, 4°C, 10 min). The supernatant was then loaded into injection needles and injected into HeLa cells. After microinjection, cells were incubated for 4 h. They were then processed for immunofluorescence as described above.

Assay of CPA Activity on Permeabilized Cells

Cells grown for 2 days on glass coverslips were permeabilized with warm OPT buffer [80 mmol/L PIPES, 1 mmol/L EGTA, 1 mmol/L $MgCl_2$, 0.5% Triton X-100, 10% glycerol (pH 6.8)]. OPT buffer permeabilizes cells while preserving intact microtubules (28). CPA (0.5 μg/mL) diluted in warm OPT buffer was added with or without inhibitory compounds (1 mmol/L). Cells were incubated for 15 min at 37°C and then fixed and processed for immunofluorescence as described above.

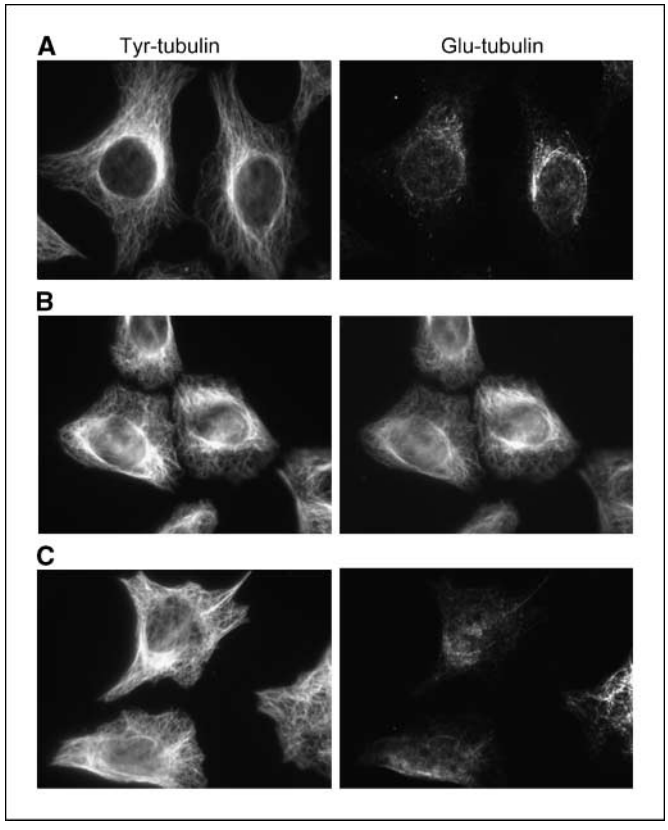

Figure 2. Immunofluorescence analysis of the effect on paclitaxel-induced tubulin detyrosination of natural extract fractions selected by the high-throughput screening assay. HeLa cells were incubated for 2 h with DMSO (*A*), 5 μmol/L paclitaxel (*B*), or 5 μmol/L paclitaxel combined with an active fraction (*C*). Cells were then fixed, double stained with Tyr-tubulin and Glu-tubulin antibodies as indicated, and processed for immunofluorescence as described in Materials and Methods.

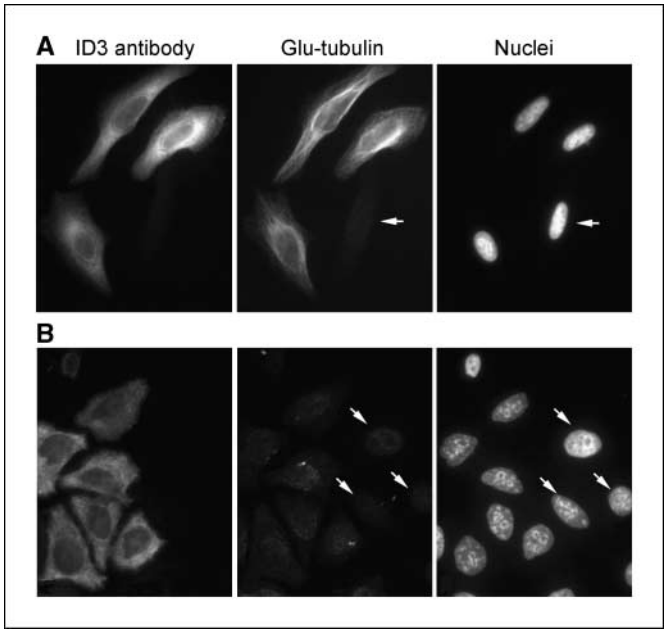

Figure 3. Analysis of the effect of natural extract fractions on TCP activity revealed by accumulation of Glu-tubulin after ID3 microinjection. HeLa cells were microinjected with the TTL inhibitory antibody ID3, incubated for 4 h with (*A*) or without (*B*) a TCP-inhibiting fraction, fixed, and processed for immunofluorescence as described in Materials and Methods. Cells were triple stained using an antimouse Cy3-conjugated antibody to mark ID3 microinjected cells, L4 antibody and Alexa Fluor 488–conjugated secondary antibody to visualize Glu-tubulin, and Hoechst 33258 to visualize nuclei. In control cells (*A*), Glu-tubulin is generated in the microinjected cells and not in a nonmicroinjected cell (*arrow*), which can be localized thanks to Hoechst 33258 staining. *B,* example of a fraction showing an inhibitory effect on TCP activity. In the presence of such a fraction, the level of Glu-tubulin is as low in microinjected cells as in nonmicroinjected cells (*arrows*).

Results

Screen for chemicals that decrease paclitaxel-induced tubulin detyrosination. The rationale of the assay relies on the substrate properties of TCP and TTL. TTL, the enzyme that catalyzes the tubulin tyrosination reaction, adds tyrosine to soluble, detyrosinated tubulin and does not react with tubulin once it is assembled into microtubules (3, 29–31). TCP is likely to prefer polymerized substrate, and its binding to microtubules may be required for its function (30, 32, 33). TCP acts slowly on microtubules, whereas TTL recharges Glu-tubulin quickly on release from microtubules (30). As a consequence of the substrate specificity of TTL and of the kinetic differences of TTL and TCP, Tyr-tubulin is the main component of dynamic microtubules, being the dominant tubulin variant in cycling cells *in vitro*, whereas Glu-tubulin is a marker of long-lived stable microtubules (3, 30, 34–36). Depending on the cell type, these Glu-microtubules either are not detectable or represent a small subpopulation of the cellular microtubules. In HeLa cells, these Glu-microtubules are almost absent (28). However, they do accumulate on paclitaxel treatment, indicating that TCP is active in these cells. We set up an assay amenable to automation, in which TCP inhibitors were selected according to their ability to inhibit accumulation of Glu-tubulin in HeLa cells with paclitaxel-stabilized microtubules. Briefly, compounds were added to HeLa cells grown in 96-well microplates. Cells were treated with paclitaxel immediately after addition of the compounds. After 2 h of incubation, cells were rinsed, fixed, and permeabilized with methanol. Glu-tubulin was then quantified by immunoluminescence using a specific antibody (6, 28). The Glu-tubulin signal obtained after treatment of the cells with paclitaxel alone was defined as 0% of inhibition, whereas the basal Glu-tubulin signal obtained after treatment with only DMSO was taken as 100% of inhibition. The different steps of the assay are illustrated in Fig. 1.

Screening of partially purified natural extracts. A total of 23,904 partially purified extracts, corresponding to 3,252 natural species (81.5% plants, 2.5% insects, and 16% marine organisms), was screened for potential TCP-inhibiting activity using the above described assay (Fig. 1). Among these, 268 extracts (1.1% hit rate) were scored as positive, showing >50% of inhibition. However, in such a cell-based assay, a lowered Glu-tubulin signal could result from a global toxic effect of the extracts on the cells. We thus assayed the extract cytotoxicity using a MTT assay. A subset of 127 extracts showed some cytotoxicity after 2 h of incubation on the cells and was discarded. Among the 141 remaining extracts, 49 extracts showed an apparent inhibitory activity superior to 70%. These most active extracts were set aside for further characterization.

Bioguided fractionation and identification of TCP inhibitors. The 49 extracts were submitted to fractionation by combining chromatographies (normal and reverse C18 phases), and each fraction was tested again using several different biological complementary assays (bioguided fractionation). The aim of these other assays was to discriminate between false- and true-positive compounds.

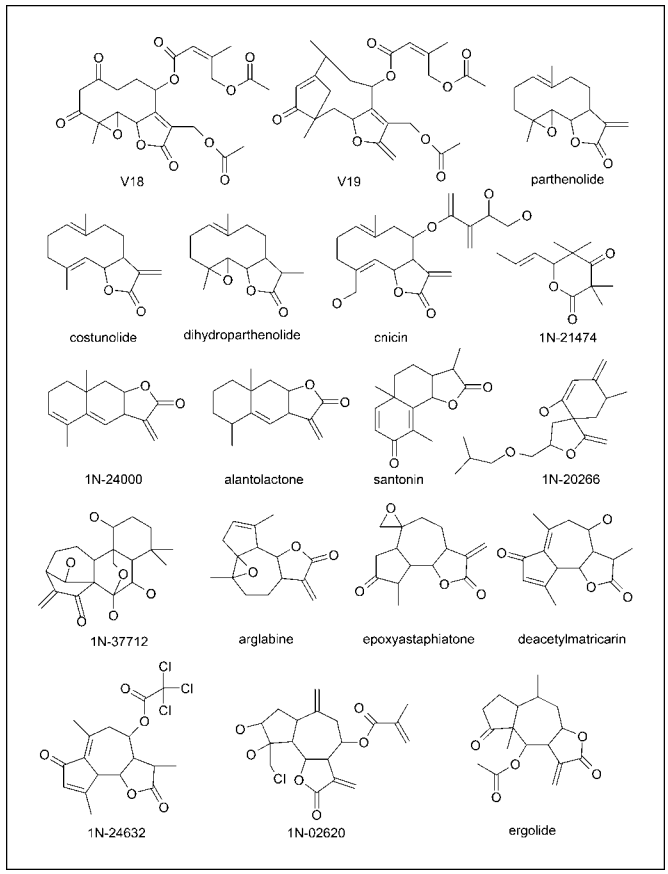

Figure 4. Chemical structures of the two compounds (V18 and V19), isolated from *V. perrottetii*, and of the 17 structural analogues tested.

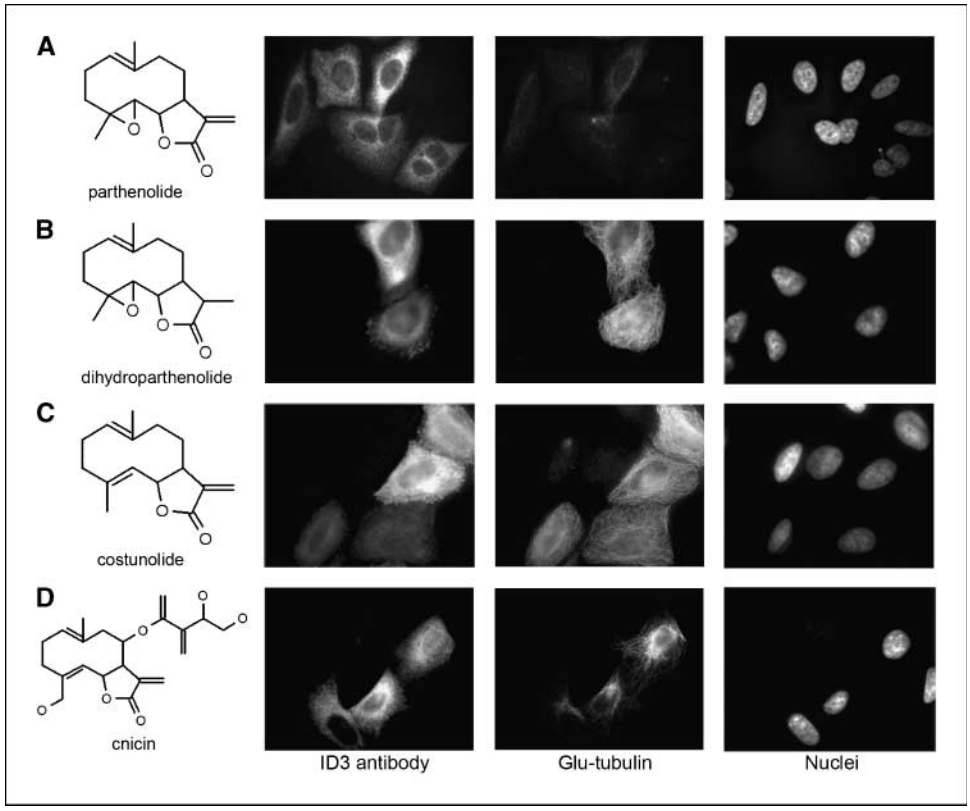

Figure 5. Comparison of the effect of several structural analogues of V18 and V19 on TCP activity evaluated after ID3 microinjection. HeLa cells were microinjected with the TTL inhibitory antibody ID3 and incubated for 4 h with the different compounds as indicated. They were then fixed and processed for immunofluorescence as described in Materials and Methods. Cells were triple stained using an antimouse Cy3-conjugated antibody to mark ID3 microinjected cells, L4 antibody and Alexa Fluor 488–conjugated secondary antibody to visualize Glu-tubulin, and Hoechst 33258 to visualize nuclei as indicated.

All fractions were first screened using tubulin immunofluorescence microscopy to examine their effects on microtubule structure (data not shown). Fractions able to depolymerize the microtubule network were classed as potential false positive. Indeed, such compounds could have competed with paclitaxel during the high-throughput screening assay and thus led to a diminished Glu-tubulin signal that does not result to TCP inhibition. Such depolymerizing fractions were discarded, and only fractions showing no detectable effect on the microtubule network were kept. These last fractions were checked for their inhibitory effect on paclitaxel-induced tubulin detyrosination using tubulin immunofluorescence microscopy (Fig. 2). When cells were only treated with DMSO (Fig. 2*A*), the Glu-microtubules represented a small subpopulation of cellular microtubules as expected. After paclitaxel treatment (Fig. 2*B*), Glu-microtubules did accumulate, reflecting TCP action on stabilized microtubules. This accumulation was prevented when cells were treated with the fractions selected by the screening strategy, together with paclitaxel (Fig. 2*C*), although paclitaxel still exerted its stabilizing effect as indicated by the presence of tyrosinated microtubule bundles.

Finally, the inhibitory effect of the remaining fractions was investigated with another assay of TCP activity using microinjection experiments (Fig. 3). In such an assay, TCP activity is assessed after blocking TTL activity in cells by microinjection of ID3, a monoclonal antibody directed against the active site of TTL (29, 37). The activity of TCP is revealed in injected cells by the resulting accumulation of Glu-tubulin (Fig. 3*A*). In the presence of a TCP-inhibiting fraction, such an accumulation does not occur. In that case, the level of detyrosinated tubulin (Fig. 3*B*) is as low in microinjected cells as in non-microinjected cells, which can be localized thanks to Hoechst 33258 staining of the nuclei.

The overall process allowed the selection of an extract from *Vernonia perrottetii*, and this led to the isolation of two compounds (V18 and V19). Their structures were established by analysis of their NMR data and comparison with published values. These compounds were structurally related sesquiterpene lactones (V18 and V19; Fig. 4). They showed a potent TCP inhibitory activity, as assessed by ID3 microinjection experiment, for a concentration of 10 μmol/L.

Preliminary structure-activity relationships. We tested the effect of 17 available structural analogues of the active compounds (Fig. 4), at a final concentration of 20 μmol/L, on TCP activity evaluated by ID3 microinjection experiments. Among these compounds, we found that only the known anti-inflammatory sesquiterpene lactone parthenolide, originally extracted from feverfew *Tanacetum parthenium*, and, to a much lesser extent, cnicin displayed a TCP inhibitory activity (Fig. 5*D*).

Parthenolide showed a similar TCP inhibitory activity than the two compounds isolated from *V. perrottetii* (Fig. 5*A*). This indicates that the C8 lateral chain, present on V18 and V19, is not necessary for TCP inhibitory activity.

There are strong indications that alkylation of cysteine(s) is a general mechanism for sesquiterpene lactones, which possess α,β-unsaturated carbonyl structures, such as α-methylene lactones (24). These structural elements preferably react with nucleophiles, especially sulfhydryl groups, by a Michael-type addition. To test the importance of such an unsaturated α, β-lactone, we synthesized dihydroparthenolide and assayed it for TCP inhibition. Dihydroparthenolide did not show any activity (Fig. 5*B*), indicating that the unsaturated α, β-lactone is in fact necessary for TCP inhibitory activity. However, we found that the presence of the unsaturated α, β-lactone, even if it is necessary, is not sufficient for TCP inhibition. For instance, costunolide showed no TCP inhibitory activity

(Fig. 5*C*). Costunolide possesses an unsaturated α, β-lactone and differs from parthenolide by the lost of an epoxide function. This underlies the importance of the epoxide function in TCP inhibitory activity. The replacement of this epoxide function by an alcohol (cnicin) leads to a partial loss of activity (Fig. 5*D*).

We tested the cytotoxicity of parthenolide and of the compounds V18 and V19. HeLa cells were exposed to increasing concentrations of these molecules, and cytotoxicity was measured after 48 h using MTT assay. We found that parthenolide, V18, and V19 had similar cytotoxic properties with an IC_{50} of 8, 3.5, and 7.1 μmol/L, respectively.

Does the observed parthenolide inhibition of TCP activity result from NF-κB inhibition? One well-described activity of parthenolide is its potent anti-inflammatory effect, which is mainly achieved through its inhibitory effects on NF-κB activation. Thus, the observed TCP inhibition by parthenolide could actually be an indirect result of NF-κB inhibition. Costunolide, an also known NF-κB inhibitor, has no effect on TCP activity, indicating that TCP inhibition does not result from NF-κB inhibition. However, this conclusion remains uncertain due to the different NF-κB inhibitory potencies of parthenolide and costunolide (24). To get insight into that question, we tested the effect of sulindac, an inhibitor of NF-κB activation (38, 39) that is not structurally related to parthenolide or costunolide, on TCP activity. We found that 1 mmol/L sulindac has no inhibitory effect on the generation of Glu-tubulin induced by ID3 microinjection (data not shown). This result strongly shows that parthenolide inhibition of TCP activity is independent of NF-κB inhibition.

Specific action of parthenolide on TCP. *In vitro*, CPA is able to excise the COOH-terminal tyrosine of tubulin as well as does TCP in cells (40). We tested if parthenolide could also inhibit CPA using a cell-based assay of CPA activity. In such an assay, the effect of the application of exogenous CPA on the cellular microtubule network is observed by the generation of Glu-tubulin in permeabilized cells. The buffer used for the permeabilization preserves microtubule network (28). In the absence of CPA, the microtubule network is predominantly composed of Tyr-tubulin, whereas Glu-tubulin is almost absent (Fig. 6*A*).

After an exposition of 15 min to CPA, the Glu-tubulin staining is largely enhanced, extending to the entire microtubule network (Fig. 6*B*). This augmentation is prevented when orthophenanthroline is added to cells in combination with CPA (Fig. 6*C*). Orthophenanthroline is a known CPA inhibitor with no effect on TCP (12). When cells are exposed with CPA in combination with parthenolide, the Glu-tubulin staining is the same as the Glu-tubulin staining observed with CPA alone (Fig. 6*D*). Although parthenolide is a reactive compound because of its unsaturated α, β-lactone, this result shows that it has no effect on CPA even at the highest concentration (1 mmol/L) tested.

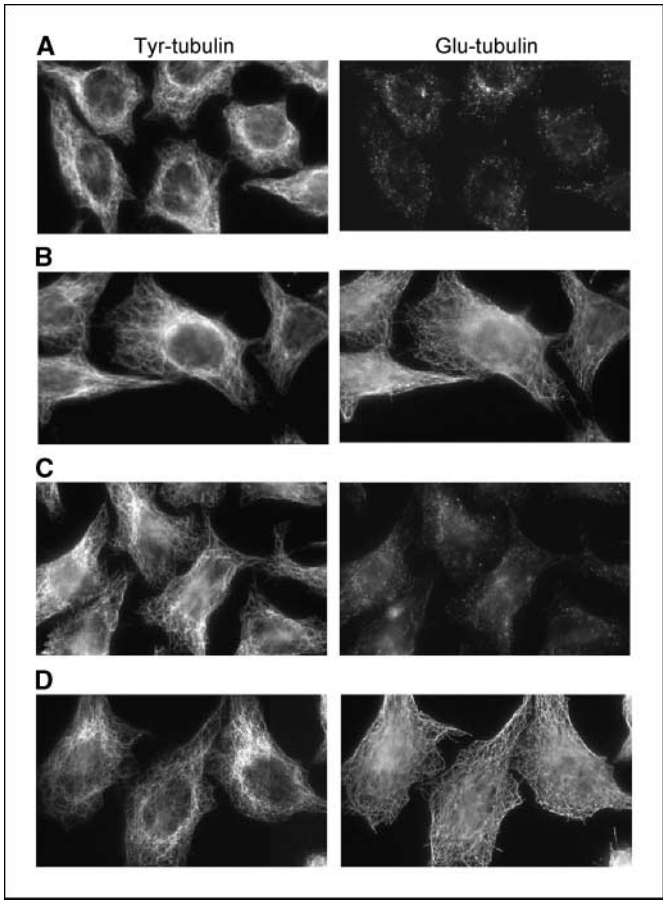

Figure 6. Test of the effect of parthenolide on CPA. Permeabilized cells were exposed to buffer alone (*A*) or to CPA (*B–D*) alone (*B*) or in combination with orthophenanthroline (*C*) or with parthenolide (*D*) as described in Materials and Methods. After 15 min of exposition, cells were fixed and processed for immunofluorescence. Cells were double stained with Tyr-tubulin antibody and Glu-tubulin antibody as indicated.

Discussion

By screening a natural extract library on a cell-based assay of TCP activity, we have isolated two structurally related sesquiterpene lactones that produce a strong inhibition on cellular TCP activity.

When searching for therapeutic agents, cell-based assays are particularly valuable because they select not only for activity against a particular molecular target but also for other desirable properties, such as the ability to permeate cells and to retain activity in tissue culture medium and in cells (23). Moreover, by screening for inhibitors on the entire cell, multiple potential targets, direct or indirect, are tested, allowing the cell to dictate the best target.

Although the screen that we set up could lead to the selection of some false positives, the overall strategy was discriminative and led to the isolation of only two compounds. This is noteworthy as regards the high number of compounds tested. We have screened extracts, which could be considered as mixtures of natural substances. Thus, the true number of different compounds tested is much higher than 23,904 (i.e., the number of extracts tested).

We tested several commercially available analogues of the compounds that were isolated by the screening procedure and found that parthenolide, but not the closely related compound costunolide, has also a potent inhibitory effect on TCP. Parthenolide, as well as other sesquiterpene lactones, contains an α-methylene-β-lactone moiety, which is highly reactive with cellular thiols, resulting in alkylation of sulfydryl residues through Michael-type addition. We found that this α-methylene-β-lactone moiety was indispensable for the inhibitory effect of parthenolide on TCP. If the observed inhibitory effect of parthenolide is the consequence of a direct reaction of parthenolide with TCP, this result indicates that TCP could belong to the class of cysteine proteases. Moreover, as parthenolide has no effect on CPA and as

known metalloproteinases inhibitors have no effect on TCP (12), it seems that TCP is not a metalloproteinase.

Numerous bioactivities, probably as a consequence of its high reactivity, have been described for parthenolide and other related sesquiterpene lactones. These bioactivities include, for example, anti-inflammatory effect through inhibition of NF-κB activation (41) and signal transducers and activators of transcription signaling pathway (42) or induction of apoptosis through several different mechanisms, such as caspase activation and mitochondrial dysfunction (43, 44). Contrary to the panel of actions described for sesquiterpene lactones, TCP inhibition looks to be a specific action of parthenolide and of the two *Vernonia* compounds selected.

We have shown that the inhibitory effect of parthenolide on TCP does not seem to result from the parthenolide action on NF-κB pathway. However, we cannot exclude that TCP inhibition is an indirect consequence of an action of parthenolide on another known or unknown target. For example, it cannot be excluded that parthenolide inhibits regulating enzymes, such as kinases or phosphatases. It has been shown that inhibitors of serine/threonine phosphatases seem to dissociate TCP from microtubules (45). Such an inhibition could thus represent an indirect form of TCP inhibition.

Our initial aim was to use the inhibitor selected by the screening procedure as a hook, in an attempt to isolate TCP, as it has been successfully done in some chemical genetic approaches. However, because of its high reactivity and its numerous targets, parthenolide is no suitable for such a strategy. We are currently testing other chemical libraries in an attempt to isolate a compound more convenient for TCP purification.

The anticancer potential of parthenolide has been described both *in vitro* (43, 46–49) and on animal models (44, 50). Moreover, it has been shown that parthenolide could reduce metastasis (50). We believe that TCP inhibition, which could antagonize the abnormal accumulation of detyrosinated tubulin in tumor cells, could be one of the mechanisms underlying the anticancer and antimetastatic properties of parthenolide. Because parthenolide has shown safety in phase I clinical trials, our results have direct clinical relevance.

Acknowledgments

Received 10/11/2006; revised 12/22/2006; accepted 1/5/2007.

Grant support: Alliance des Recherches sur le Cancer, an Association pour la Recherche sur le Cancer initiative, and Rhône-Alpes Region. X. Fonrose is a recipient of a fellowship from Association pour la Recherche sur le Cancer.

The costs of publication of this article were defrayed in part by the payment of page charges. This article must therefore be hereby marked *advertisement* in accordance with 18 U.S.C. Section 1734 solely to indicate this fact.

We thank Dr. Jacques Fahy (Institut de Recherche Pierre Fabre, Boulogne, France) for parthenolide hydrogenation experiment, Delphine Scokaert for her contribution in the initial step of this project, Catherine Pillet for technical assistance, and Muriel Batut and Stephanie Brillant for the isolation of the compounds from *Vernonia*.

References

1. Barra HS, Arce CA, Argarana CE. Posttranslational tyrosination/detyrosination of tubulin. Mol Neurobiol 1988;2:133–53.
2. Ersfeld K, Wehland J, Plessmann U, et al. Characterization of the tubulin-tyrosine ligase. J Cell Biol 1993;120:725–32.
3. Lafanechere L, Job D. The third tubulin pool. Neurochem Res 2000;25:11–8.
4. Erck C, Peris L, Andrieux A, et al. A vital role of tubulin-tyrosine-ligase for neuronal organization. Proc Natl Acad Sci U S A 2005;102:7853–8.
5. Lafanechere L, Courtay-Cahen C, Kawakami T, et al. Suppression of tubulin tyrosine ligase during tumor growth. J Cell Sci 1998;111:171–81.
6. Mialhe A, Lafanechere L, Treilleux I, et al. Tubulin detyrosination is a frequent occurrence in breast cancers of poor prognosis. Cancer Res 2001;61:5024–7.
7. Kato C, Miyazaki K, Nakagawa A, et al. Low expression of human tubulin tyrosine ligase and suppressed tubulin tyrosination/detyrosination cycle are associated with impaired neuronal differentiation in neuroblastomas with poor prognosis. Int J Cancer 2004;112:365–75.
8. Soucek K, Kamaid A, Phung AD et al. Normal and prostate cancer cells display distinct molecular profiles of α-tubulin posttranslational modifications. Prostate 2006;66:954–65.
9. Badin-Larcon AC, Boscheron C, Soleilhac JM, et al. Suppression of nuclear oscillations in *Saccharomyces cerevisiae* expressing Glu tubulin. Proc Natl Acad Sci U S A 2004;101:5577–82.
10. Peris L, Thery M, Faure J, et al. Tubulin tyrosination is a major factor affecting the recruitment of CAP-Gly proteins at microtubule plus ends. J Cell Biol 2006;174:839–49.
11. Vasiliev JM, Omelchenko T, Gelfand IM, et al. Rho overexpression leads to mitosis-associated detachment of cells from epithelial sheets: a link to the mechanism of cancer dissemination. Proc Natl Acad Sci U S A 2004;101:12526–30.
12. Webster DR. Tubulinyl-Tyr carboxypeptidase. In: Barrett AJ, Rawlings ND, Woessner JF, editors. Handbook of proteolytic enzymes. London: Academic Press; 1998.
13. Khawaja S, Gundersen GG, Bulinski JC. Enhanced stability of microtubules enriched in detyrosinated tubulin is not a direct function of detyrosination level. J Cell Biol 1988;106:141–9.
14. Stockwell BR. Chemical genetics: ligand-based discovery of gene function. Nat Rev Genet 2000;1:116–25.
15. Bredel M, Jacoby E. Chemogenomics: an emerging strategy for rapid target and drug discovery. Nat Rev 2004;5:262–75.
16. Mitchison T. Toward pharmacological genetics. Chem Biol 1994;1:3–6.
17. Stockwell BR, Haggarty SJ, Schreiber SL. High-throughput screening of small molecules in miniaturized mammalian cell-based assays involving post-translational modifications. Chem Biol 1999;6:71–83.
18. Crews CM, Spittgerber U. Chemical genetics: exploring and controlling cellular processes with chemical probes. Trends Biochem Sci 1999;24:317–20.
19. Burdine L, Kodadek T. Target identification in chemical genetics: the (often) missing link. Chem Biol 2004;11:593–7.
20. Mayer TU, Kapoor TM, Haggarty SJ, et al. Small molecule inhibitor of mitotic spindle bipolarity identified in a phenotype-based screen. Science 1999;286:971–4.
21. Peterson JR, Lokey RS, Mitchison TJ, et al. A chemical inhibitor of N-WASP reveals a new mechanism for targeting protein interactions. Proc Natl Acad Sci U S A 2001;98:10624–9.
22. Carey KL, Westwood NJ, Mitchison TJ, et al. A small-molecule approach to studying invasive mechanisms of *Toxoplasma gondii*. Proc Natl Acad Sci U S A 2004;101:7433–8.
23. Roberge M, Cinel B, Anderson HJ, et al. Cell-based screen for antimitotic agents and identification of analogues of rhizoxin, eleutherobin, and paclitaxel in natural extracts. Cancer Res 2000;60:5052–8.
24. Siedle B, Garcia-Pineres AJ, Murillo R, et al. Quantitative structure-activity relationship of sesquiterpene lactones as inhibitors of the transcription factor NF-κB. J Med Chem 2004;47:6042–54.
25. Kwok BH, Koh B, Ndubuisi MI, et al. The anti-inflammatory natural product parthenolide from the medicinal herb Feverfew directly binds to and inhibits IκB kinase. Chem Biol 2001;8:759–66.
26. Zhang JH, Chung TD, Oldenburg KR. A simple statistical parameter for use in evaluation and validation of high throughput screening assays. J Biomol Screen 1999;4:67–73.
27. Tully LE, Carson MS, McMurry TBH. A novel sesquiterpene lactone from *Vernonia erinacea*. Tetrahedron Lett 1987;28:5925–8.
28. Vassal E, Barette C, Fonrose X, et al. Miniaturization and validation of a sensitive multiparametric cell-based assay for the concomitant detection of microtubule-destabilizing and microtubule-stabilizing agents. J Biomol Screen 2006;11:377–89.
29. Wehland J, Weber K. Tubulin-tyrosine ligase has a binding site on β-tubulin: a two-domain structure of the enzyme. J Cell Biol 1987;104:1059–67.
30. Wehland J, Weber K. Turnover of the carboxy-terminal tyrosine of α-tubulin and means of reaching elevated levels of detyrosination in living cells. J Cell Sci 1987;88:185–203.
31. Arce CA, Hallak ME, Rodriguez JA, et al. Capability of tubulin and microtubules to incorporate and to release tyrosine and phenylalanine and the effect of the incorporation of these amino acids on tubulin assembly. J Neurochem 1978;31:205–10.
32. Gundersen GG, Khawaja S, Bulinski JC. Postpolymerization detyrosination of α-tubulin: a mechanism for subcellular differentiation of microtubules. J Cell Biol 1987;105:251–64.
33. Kreis TE. Microtubules containing detyrosinated tubulin are less dynamic. EMBO J 1987;6:2597–606.
34. Gundersen GG, Kalnoski MH, Bulinski JC. Distinct populations of microtubules: tyrosinated and nontyrosinated α tubulin are distributed differently *in vivo*. Cell 1984;38:779–89.
35. Schulze E, Asai DJ, Bulinski JC, et al. Posttranslational modification and microtubule stability. J Cell Biol 1987;105:2167–77.
36. Westermann S, Weber K. Post-translational modifications regulate microtubule function. Nat Rev Mol Cell Biol 2003;4:938–47.
37. Erck C, Frank R, Wehland J. Tubulin-tyrosine ligase, a long-lasting enigma. Neurochem Res 2000;25:5–10.

38. Karin M, Yamamoto Y, Wang QM. The IKK NF-κB system: a treasure trove for drug development. Nat Rev Drug Discov 2004;3:17–26.
39. Yamamoto Y, Yin MJ, Lin KM, et al. Sulindac inhibits activation of the NF-κB pathway. J Biol Chem 1999;274: 27307–14.
40. Paturle L, Wehland J, Margolis RL, et al. Complete separation of tyrosinated, detyrosinated, and nontyrosinatable brain tubulin subpopulations using affinity chromatography. Biochemistry 1989;28: 2698–704.
41. Hehner SP, Hofmann TG, Droge W, et al. The antiinflammatory sesquiterpene lactone parthenolide inhibits NF-κB by targeting the IκB kinase complex. J Immunol 1999;163:5617–23.
42. Sobota R, Szwed M, Kasza A, et al. Parthenolide inhibits activation of signal transducers and activators of transcription (STATs) induced by cytokines of the IL-6 family. Biochem Biophys Res Commun 2000;267: 329–33.
43. Zhang S, Won YK, Ong CN, et al. Anti-cancer potential of sesquiterpene lactones: bioactivity and molecular mechanisms. Curr Med Chem Anticancer Agents 2005;5:239–49.
44. Won YK, Ong CN, Shi X, et al. Chemopreventive activity of parthenolide against UVB-induced skin cancer and its mechanisms. Carcinogenesis 2004;25: 1449–58.
45. Contin MA, Purro SA, Bisig CG, et al. Inhibitors of protein phosphatase 1 and 2A decrease the level of tubulin carboxypeptidase activity associated with microtubules. Eur J Biochem 2003;270:4921–9.
46. Zhang S, Ong CN, Shen HM. Critical roles of intracellular thiols and calcium in parthenolide-induced apoptosis in human colorectal cancer cells. Cancer Lett 2004;208:143–53.
47. Yip-Schneider MT, Nakshatri H, Sweeney CJ, et al. Parthenolide and sulindac cooperate to mediate growth suppression and inhibit the nuclear factor-κB pathway in pancreatic carcinoma cells. Mol Cancer Ther 2005;4: 587–94.
48. Ralstin MC, Gage EA, Yip-Schneider MT, et al. Parthenolide cooperates with NS398 to inhibit growth of human hepatocellular carcinoma cells through effects on apoptosis and G_0-G_1 cell cycle arrest. Mol Cancer Res 2006;4:387–99.
49. Kim JH, Liu L, Lee SO, et al. Susceptibility of cholangiocarcinoma cells to parthenolide-induced apoptosis. Cancer Res 2005;65:6312–20.
50. Sweeney CJ, Mehrotra S, Sadaria MR, et al. The sesquiterpene lactone parthenolide in combination with docetaxel reduces metastasis and improves survival in a xenograft model of breast cancer. Mol Cancer Ther 2005;4:1004–12.